

Piezoelectric field around threading dislocation in GaN determined on the basis of high-resolution transmission electron microscopy image

G. MACIEJEWSKI*, S. KRET† & P. RUTERANA‡

*Institute of Fundamental Technological Research PAS, 00-049 Warsaw, ul. Świętokrzyska 21, Poland

†Institute of Physics PAS, 02-668 Warsaw, Al. Lotników 32/46, Poland

‡SIFCOM UMR 6176 CNRS-ENSICAEN, 6 Boulevard du Marechal Juin, 14050 Caen Cedex, France

Key words. Gallium nitride, piezoelectricity, thin films, threading dislocations, transmission electron microscopy.

Summary

A new method of determining the piezoelectric field around dislocations from high-resolution transmission electron microscopy images is presented. In order to determine the electrical potential distribution near a dislocation core, we used the distortion field, obtained using the geometrical phase method and the non-linear finite element method. The electrical field distribution was determined taking into account the inhomogeneous strain distribution, finite geometry of the sample and the full couplings between elastic and electrical fields. The results of the calculation for a transmission electron microscopy thin sample are presented.

Introduction

In recent years many attempts have been made to experimentally determine both the electrical field around dislocations and charges accumulated at dislocation cores (DCs). In particular, the electron holography method has been used to study charge accumulation on dislocations in GaN as presented by Cherns & Jiao (2001). In the case of n-GaN, the measured change in the inner potential between a DC region and a region outside the DC reached approximately -3 V. The same method was applied by Cai & Ponce (2002) in their report on undoped GaN where the measured change in the inner potential was around -1.2 V. Contrary to the above results, Im *et al.* (2001) obtained positive changes in the case of n-GaN using ballistic electron emission microscopy and the electrostatic modelling of the local potential profile close to a charged threading dislocation. An asymmetric profile of the potential with respect to the DC was also reported. Krtschil *et al.* (2003),

using scanning surface potential microscopy, studied different dopings in GaN single layers vs. the dislocation-related surface depression and their charge states. The results of their experiments were not conclusive. In some samples, the dislocations were negatively charged and in others they were neutral, and even samples could exhibit both charged and electrically inactive dislocation pits. These determined total electrostatic potential distributions around threading dislocations, which have still not been established, must be the result of overlapping of the potential due to charged cores and due to both the inhomogeneous strain field around a DC and piezoelectricity. These two sources of an electrical potential cannot be uncoupled, as yet, in an experimental manner. The asymmetry of the potential field reported by Im *et al.* (2001) may result from the large piezoelectric effect associated with a large strain near a DC.

In this study, we propose a new method to determine the piezoelectric field distribution around threading dislocations in a [0001]-GaN epilayer, through numerical simulation using the geometric phase method determination of the strain field in nanoscale and the non-linear finite element method.

Determination of displacements

The planar-view transmission electron microscopy sample of a GaN epilayer on a (0001) sapphire substrate was prepared by mechanical polishing followed by ion milling. High-resolution transmission electron microscopy was carried out using a Topcon 002B microscope operating at 200 kV, with a point-to-point resolution of 0.19 nm. All of the dislocations in Fig. 1 have the same Burgers vector $1/3\langle 2\bar{1}\bar{1}0 \rangle$ parallel to the X-axis and their dislocation lines (DLs) are parallel to the incident electron beam. Processing of experimental images was performed using routines written in Analytical Language for Images of Optimas graphical environment (Media Cybernetics, 1999). In our procedure, the phase images were calculated for the $(0\bar{1}\bar{1}0)$ and $(1\bar{1}00)$ lattice periodicities.

Correspondence to: Dr G. Maciejewski. Tel: +48-22-826 1281; Fax: +48-22-826 9815; e-mail: gmaciej@ippt.gov.pl

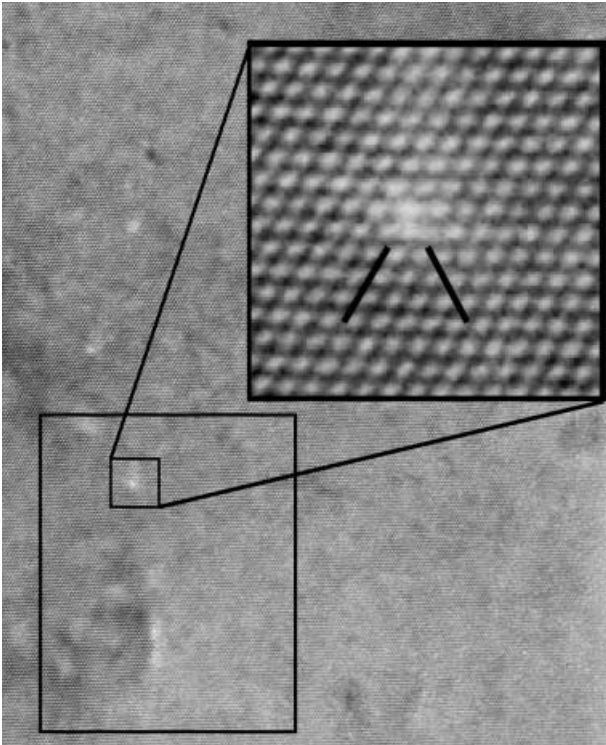


Fig. 1. High-resolution transmission electron microscopy image of the GaN epilayer in the [0001] zone axis with zoomed dislocation region; the black frame shows the area used for the calculation.

As was shown by Kret *et al.* (2001), for foil thickness and defocus windows in which the first 'inverse contrast condition' is valid, the strain field extracted from high-resolution transmission electron microscopy images is in agreement with that calculated by atomistic relaxation. Using our microscope, this was obtained in the defocus window of $-50 \dots -60$ nm and foil thickness range of $t = 5-25$ nm for the GaN crystal along the [0001] zone axis. The lattice distortions tensor $\beta(x,y)$ was determined using the geometrical phase method (Hytch *et al.*, 2003). The components of the distortion tensor, determined for the area in the black frame in Fig. 1, are shown in Fig. 2. The details of the image contrast near a DC can be seen in the zoomed image in Fig. 1.

Determination of the electrical field

GaN is a strongly piezoelectric crystal and, for this reason, the elastic and electrical fields should be constitutively coupled. As large strains occur near a DC, the large deformation formalism is used (Basar & Weichert, 2000). The direct piezoelectric effect states that strain applied to a material induces a change of charge distribution. Thus, the constitutive equation for the second Piola-Kirchhoff stress tensor S of the linear piezoelectric material is given by

$$S = CE_e - e^T E \quad (1)$$

in which C , E_e , e^T and E are the fourth-order elastic moduli tensor, second-order elastic strain tensor, transposition of the third-order piezoelectricity tensor and electrical field vector, respectively. The second term on the right-hand side of Eq. (1) is responsible for the piezoelectric couplings. Analogically, the constitutive equation for the electrical displacement vector D is given by

$$D = eE_e + dE + P_{sp} \quad (2)$$

in which d and P_{sp} are the second-order dielectric tensor and the vector of the spontaneous polarization. The first term on the right-hand side of Eq. (2) represents the piezoelectric couplings, whereas the third term is the residual part of the electrical displacement, i.e. the one that exists even when the strain and electrical fields vanish. The procedure was as follows. The initial strain tensor was calculated from the distortion tensor β (Le & Stumpf, 1996), which was obtained through the microscopic image analysis. It was assumed that the distortion tensor was uniform along the direction of the DLs, i.e. $\beta(x,y,z) = \beta(x,y)$ for all z . Next, for the initial strain given, the elasto-electrical equilibrium was attained by a standard numerical iteration scheme. The equilibrium equations, i.e. $Div S = 0$ and $Div D = 0$, must be satisfied [see Eqs (1) and (2)] with constraints on a surface of a body, i.e. $u = 0$ on δV^u and $\phi = 0$ on δV^ϕ , where u , ϕ , δV^u and δV^ϕ denote the displacement vector, surface free charge, surface on which the displacement vector is prescribed and surface on which the electrical charge is prescribed, respectively. In particular, the electrical potential was assumed to be equal to zero at all surfaces of the simulated area. This assumption is reasonable because charges accumulated on the surface would migrate through ions in air. However, on a surface perpendicular to the image plane, the electrical potential is usually not equal to zero and such an assumption requires the estimation of the error introduced through this assumption. In the numerical analysis, the finite element method within the Computational Templates environment was used (Korelc, 2002). The three-dimensional displacement vector and the electrical potential scalar were chosen as the nodal unknown. Only a small part of the whole sample was numerically simulated (the area in the black frame in Fig. 1). The thickness of the simulated part of the sample, perpendicular in direction to the image plane, was assumed to be 20 nm. The method used is similar to the procedure described by Kröner (1981) and Le & Stumpf (1996). In the present investigation, only the small strain formalism was replaced by the finite strain formalism and electrical parts of the governing equations were added [see Eq. (2) and the second term on the right-hand side of Eq. (1)].

An example of the results obtained is shown in Fig. 3. Figure 3(A) shows the electrical field in the Z-direction and Fig. 3(B) shows the distribution of the electrical potential. The maximum value of the electrical potential visible in Fig. 3 is around 0.012 V. A series of simulations were performed and the sensitivity of the results to a variation of an area dimension

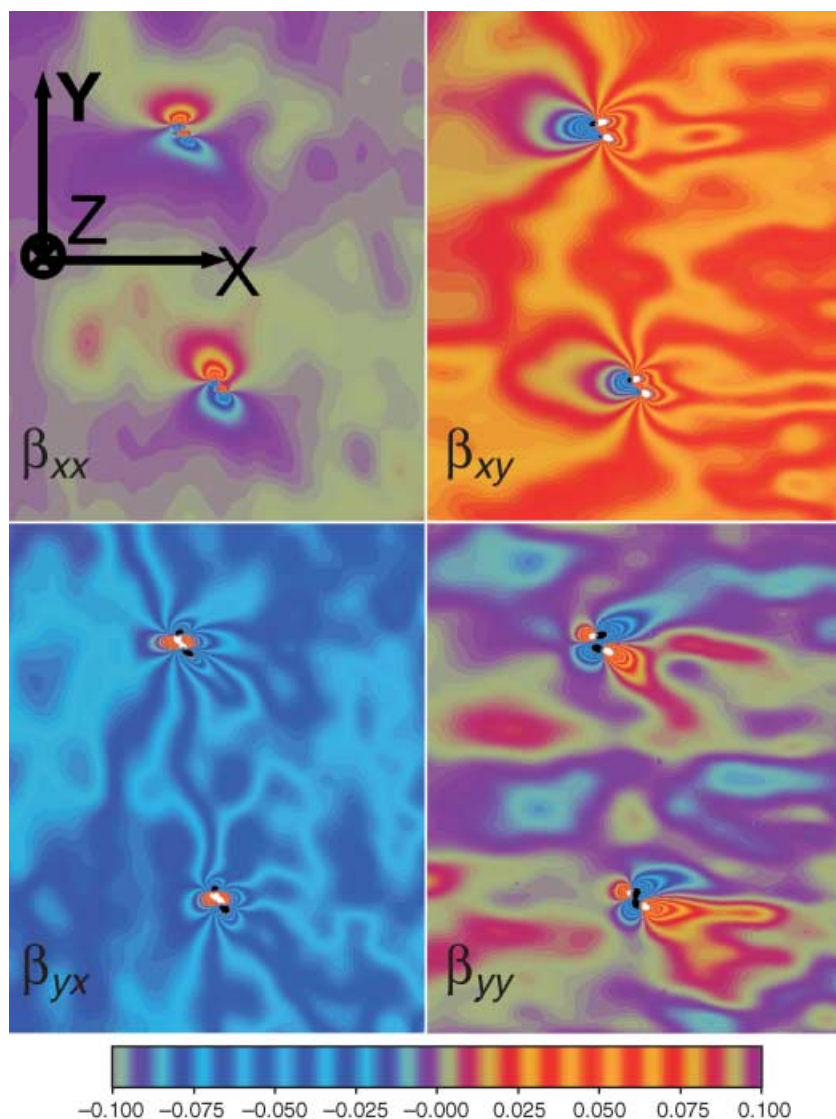


Fig. 2. Components of the lattice distortions tensor determined from the high-resolution transmission electron microscopy image. See the area in the black frame in Fig. 1.

and a sample thickness were checked. The analysed area should be as large as possible because the electrical potential at the boundary is assumed to vanish. We confirmed that if the area of simulation was twice as large as those in Fig. 1 the maximum value of the electrical potential changed by less than 5%. We also noted a strong influence of the thickness of the sample on the maximum value of the electrical potential. For instance, if the thickness of the sample was changed from 20 to 15 nm the maximum value of the electrical potential was changed by less than 1% but if the thickness was 25 nm the maximum value of the electrical potential was lowered to 0.011 V, i.e. by 8%.

Conclusions

The present experimental/computational investigation is the first attempt to determine the piezoelectric field at the

nanoscale based on the high-resolution transmission electron microscopy images. It demonstrated a relatively simple approach that can give information about the piezoelectric field distribution caused by dislocation in very thin layers. The result of simulations, some of which are presented in Fig. 3, indicated that the electrical field caused by strain can reach a value of $\pm 8 \text{ kV cm}^{-1}$. The built-in electrical field was very large because of the small dimensions of the sample. In the analysed example the electrical potential obtained reached $\pm 0.012 \text{ V}$. The values obtained were relatively small compared with the values ($\sim -3 \text{ V}$) obtained by Cherns & Jiao (2001) but, when compared with the -0.08 V obtained by Krtschil *et al.* (2003), the piezoelectric couplings seemed to be important in the problem of charge accumulation by DCs. The maximum of the electrical potential obtained using electron holography was higher in order of magnitude than the values obtained using other methods.

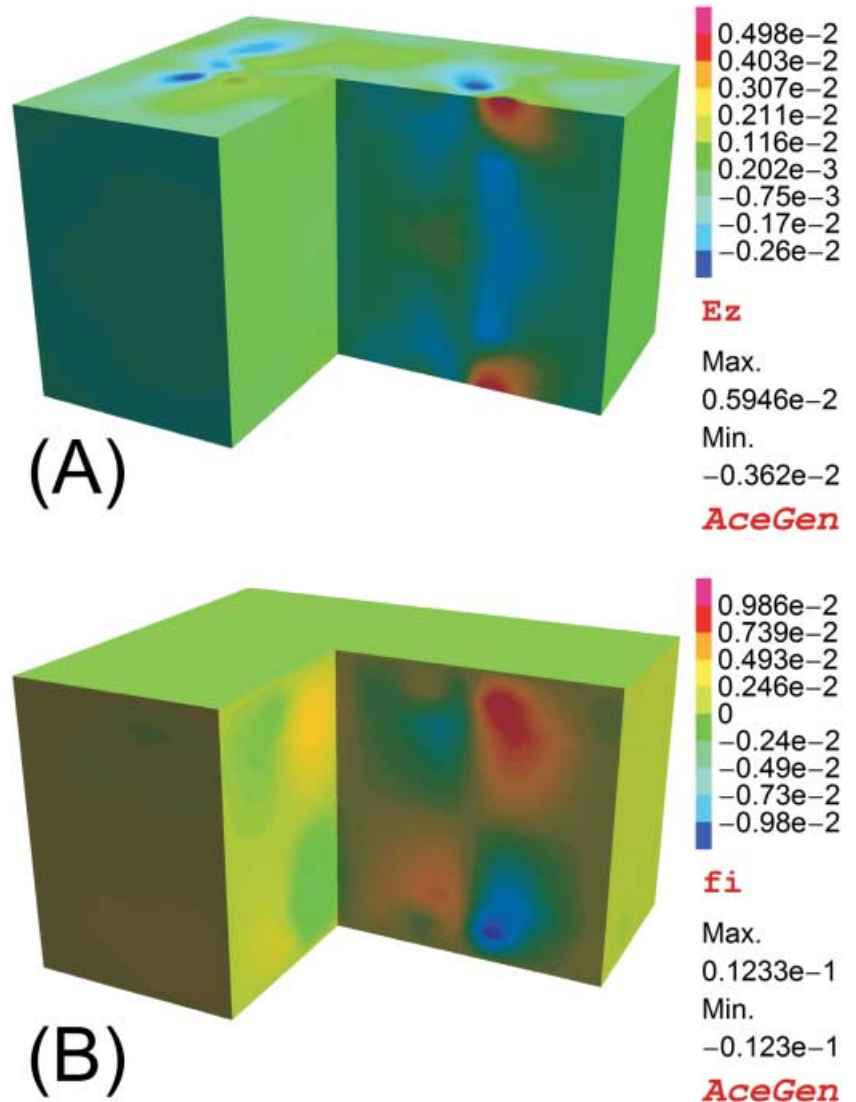


Fig. 3. Result of numerical simulation. (A) Electrical field in Z-direction (MV cm^{-1}) and (B) distribution of electric potential (V).

Acknowledgements

This work was supported by the State Committee for Scientific Research in Poland through grant no. 4 T07A 01026.

References

- Basar, Y. & Weichert, D. (2000) *Nonlinear Continuum Mechanics*. Springer-Verlag, Berlin.
- Cai, J. & Ponce, F. (2002) Determination by electron holography of the electronic charge distribution at threading dislocations in epitaxial GaN. *Phys. Stat. Sol. A – Appl. Res.* **192**, 407–411.
- Cherns, D. & Jiao, C. (2001) Electron holography studies of the charge on dislocations in GaN. *Phys. Rev. Lett.* **87**, 205504/1–205504/4.
- Hytch, M., Putaux, J. & Penisson, J. (2003) Measurement of the displacement field of dislocations to 0.03 \AA by electron microscopy. *Nature*, **423** (6937), 270–273.
- Im, H., Ding, Y., Pelz, J., Heying, B. & Speck, J. (2001) Characterization of individual threading dislocations in GaN using ballistic electron emission microscopy. *Phys. Rev. Lett.* **87**, 106802/1–106802/4.
- Korelc, J. (2002) Multi-language and multi-environment generation of nonlinear finite element codes. *Engin. Comput.* **18**, 312–327.
- Kret, S., Chen, J., Ruterana, P. & Nouet, G. (2001) Investigation of threading dislocations atomic configuration in GaN by HRTEM, geometrical phase analysis and atomistic modelling. *Microscopy of Semiconducting Materials. Institute of Physics Conference Series*, Vol. 169, p. 319. Institute of Physics Publishing, Oxford.
- Kröner, E. (1981) Continuum theory of defects. *Physics of Defects* (ed. by R. Balian, M. Klemm and J. P. Poiries), pp. 215–315. Nord-Holland, Amsterdam.
- Krtschil, A., Dadgar, A. & Krost, A. (2003) Electrical microcharacterization of dislocation-related charges in GaN-based single layers by scanning probe microscopy techniques. *J. Crystal Growth*, **248**, 542–547.
- Le, K.C. & Stumpf, H. (1996) Nonlinear continuum theory of dislocations. *Int. J. Engin. Sci.* **34**, 339–358.
- Media Cybernetics (1999) *Optimas 6.5 User Guide and Technical Reference*, 9th edn. Media Cybernetics, Silver Spring.